Cell, Vol. 119, 419–429, October 29, 2004, Copyright ©2004 by Cell Press

Formin Is a Processive Motor that Requires Profilin to Accelerate Actin Assembly and Associated ATP Hydrolysis

Stéphane Romero,[1] Christophe Le Clainche,[1] Dominique Didry,[1] Coumaran Egile,[2] Dominique Pantaloni,[1] and Marie-France Carlier[1,*]

[1]Laboratoire d'Enzymologie et Biochimie Structurales
Centre National de la Recherche Scientifique
Avenue de la Terrasse
91198 Gif-sur-Yvette
France

[2]Department of Cell Biology
Harvard Medical School
240 Longwood Avenue
Boston, Massachusetts 02115

Summary

Motile and morphogenetic cellular processes are driven by site-directed assembly of actin filaments. Formins, proteins characterized by formin homology domains FH1 and FH2, are initiators of actin assembly. How formins simply bind to filament barbed ends in rapid equilibrium or find free energy to become a processive motor of filament assembly remains enigmatic. Here we demonstrate that the FH1-FH2 domain accelerates hydrolysis of ATP coupled to profilin-actin polymerization and uses the derived free energy for processive polymerization, increasing 15-fold the rate constant for profilin-actin association to barbed ends. Profilin is required for and takes part in the processive function. Single filaments grow at least 10 μm long from formin bound beads without detaching. Transitory formin-associated processes are generated by poisoning of the processive cycle by barbed-end capping proteins. We successfully reconstitute formin-induced motility in vitro, demonstrating that this mechanism accounts for the puzzlingly rapid formin-induced actin processes observed in vivo.

Introduction

Polarized assembly of actin filaments drives cell motility. WASP-Arp2/3 and formins are two conserved, stimulus-responsive, modular protein machineries that initiate new filaments. These two machineries operate in distinct processes and are targeted to specific sites by small G proteins of the Rho family. WASP family enzymes (Machesky and Insall, 1998) use the Arp2/3 complex to generate branched actin arrays that promote extension of lamellipodia, propulsion of pathogens or endosomes, and various cell processes. Formins are recently discovered nucleators of unbranched actin filaments and are involved in motile processes such as the formation of actin cables in yeast (Evangelista et al., 1997, 2002, 2003; Ozaki-Kuroda et al., 2001; Sagot et al., 2002a), assembly of actin filaments in the cytokinetic ring (Lee et al., 1999; Kato et al., 2001; Tolliday et al., 2002; Pelham and Chang, 2002), focal adhesions and adherens junctions (Tominaga et al., 2000; Riveline et al., 2001; Kobielak et al., 2004), cell migration and ruffling (Watanabe et al., 1997; Koka et al., 2003), serum response factor activity (Copeland and Treisman, 2002), endosome motility (Gasman et al., 2003), and filopodium formation (Peng et al., 2003).

All formins contain formin homology domains FH1 and FH2. The FH2 domain is sufficient for actin nucleation in vitro, while the FH1 domain is required for in vivo function and binds profilin (Sagot et al., 2002b; Pruyne et al., 2002; Pring et al., 2003). Yeast formins Bni1p and Bnr1p and Diaphanous-related formins (mDia1, mDia2, mDia3) possess an additional G protein binding domain (Watanabe et al., 1997; Alberts, 2001; Gasman et al., 2003; Dong et al., 2003). Crystal structures of FH2 domains of formins have brought functional insight. The active FH2 domain is a stable dimer (Moseley et al., 2004). The FH2 core is monomeric and does not nucleate but caps filament barbed ends (Shimada et al., 2004). A short flexible linker between FH1 and FH2 mediates dimerization, confers FH2 its nucleating activity (Xu et al., 2004), and may play a functional role.

How formins affect actin dynamics is not fully understood. Processive actin assembly by formins had been suggested by the rapid extension of actin cables from bud sites in yeast (Yang and Pon, 2002). Recently, rapid actin-based movement of aggregates of the FH1-FH2 domain of mDia1 has been observed in vivo and in solutions of actin and profilin (Higashida et al., 2004). In vitro, the FH2 and FH1-FH2 domains of formins from *S. cerevisiae* (Bni1p, Bnr1p), *S. pombe* (Cdc12p), or mammalian cells (mDia1 and the isoforms I to V of formin 1) nucleate actin assembly. Bni1p FH2 binding to barbed ends was visualized in electron microscopy (Pruyne et al., 2002). Bni1p and mDia1 were called "leaky cappers" because in contrast to conventional cappers, which block actin association to or dissociation from the barbed ends of actin filaments, they moderately affect the rate parameters at barbed ends (Pruyne et al., 2002; Pring et al., 2003; Zigmond et al., 2003; Li and Higgs, 2003; Harris et al., 2004). However, these data are satisfactorily accommodated by the rapid equilibrium binding of Bni1p or mDia1 to barbed ends. In contrast to Bni1p and mDia1, fission yeast Cdc12p acts as a conventional strong capper but allows barbed-end growth in the presence of profilin (Kovar et al., 2003).

How can a leaky capper bound to barbed ends in rapid equilibrium find a source of free energy to become a processive motor of filament assembly? Here we demonstrate that the FH1-profilin interaction is required for processive filament assembly by FH1-FH2. FH1-FH2 increases the rate of ATP hydrolysis associated with profilin-actin assembly and uses the derived free energy as a source of energy to steer and accelerate 15-fold polymerization. In the absence of profilin, FH2 and FH1-FH2 merely work as leaky cappers. Capping proteins arrest formin-catalyzed processive growth of filaments.

Using these conclusions, rapid formin-based motility is reconstituted in vitro, thus explaining the puzzlingly

*Correspondence: carlier@lebs.cnrs-gif.fr

rapid rates of formin-induced actin processes observed in vivo.

Results

mDia1 FH1-FH2-Coated Beads Catalyze Processive Growth of Individual Actin Filaments

Polymerization assays showed that, in agreement with others (Li and Higgs, 2003; Moseley et al., 2004), both FH2 and FH1-FH2 domains of mDia1 were better nucleators of actin assembly than the homolog domains of Bni1p (Supplemental Figures S1A, S1B, and S1C at http://www.cell.com/cgi/content/full/119/3/419/DC1/). FH1-FH2 is a better nucleator than FH2. The nucleating activity depends strongly on ionic strength and was 5-fold higher at 50 mM KCl as used by Li and Higgs (2003) than at physiological ionic strength (Supplemental Figure S1D on the *Cell* website).

To mimic targeting of formin at specific cell sites, FH2 or FH1-FH2 domains were adsorbed on polystyrene beads (see Experimental Procedures). In pyrene fluorescence measurements, formin-coated beads stimulated actin assembly in the presence or absence of profilin. Although 12% of the immobilized FH1-FH2 and 39% of the immobilized FH2 were active, the activity of bead bound proteins was quantitatively identical to that of the soluble FH1-FH2 and FH2 (Figure 1A and Supplemental Figure S1E on the *Cell* website). In the fluorescence microscope, filaments formed a fluorescent actin cloud surrounding FH1-FH2-coated beads only in the presence of profilin (Figure 1B). Filaments nucleated by bead bound FH1-FH2 in the absence of profilin were free in solution, and the beads remained bare (Figure 1B). FH2-coated beads also stimulated filament assembly from actin but remained bare (Figure 1B and Supplemental Figure S1E on the *Cell* website). In conclusion, actin nuclei formed by immobilized FH2 or FH1-FH2 are released and seed filament growth in solution. In contrast, immobilized FH1-FH2 nucleates and assembles filaments in an insertional processive fashion from profilin-actin. The functional homolog of profilin, ciboulot, could not replace profilin, suggesting that the FH1-profilin interaction is involved in processive growth.

The role of profilin in formin function was further addressed by polymerization assays. Profilin and ciboulot are known to inhibit spontaneous actin nucleation (Pollard and Cooper, 1984; Boquet et al., 2000). The two proteins also identically inhibited FH2-induced nucleation (Figure 1C). On the other hand, ciboulot totally inhibited FH1-FH2-induced nucleation (Figure 1D), whereas FH1-FH2 enabled profilin-actin to nucleate filaments, albeit less efficiently than actin (Figure 1E). This effect thus depends on the interaction between the FH1 domain and profilin. The critical concentration at the formin bound barbed ends was not affected by either profilin or ciboulot, as observed with free barbed ends (Figures 1D and 1E and Supplemental Figure S2A on the *Cell* website).

The above data suggest that, in contrast to a previously proposed model (Zigmond, 2004 for review), neither FH2 nor FH1-FH2 work as processive motors of assembly of actin alone and that the association of profilin-actin with FH1-FH2 is required for processive growth. To measure how long formin stays bound to a growing filament, beads coated with FH1-FH2 at low density were placed in a solution of 0.5 μM F-actin and 4 μM profilin. Profilin-actin concentration is thus maintained at a steady-state value of 0.1 μM, while the partial critical concentration of G-actin is 0.01 μM (Pantaloni and Carlier, 1993). Fluorescence microscopy allows real-time observation of the stationary growth and detachment of individual filaments from the bead. Individual filaments nucleated at the bead surface grew at a rate of 0.4 μm/min at steady state (Figure 1F and Supplemental Movie S1 on the *Cell* website) and reached lengths of 8–15 μm, i.e., grew for periods of time of 1200 to 2500 s before detaching. The frequency of detachment of a barbed end from FH1-FH2, $K_d = 7.5 \cdot 10^{-4} \pm 1.5 \cdot 10^{-4}$ s^{-1}, was derived from the stationary length distribution of attached filaments (Figure 1G). When 0.3 μM actin depolymerizing factor (ADF) was added, filaments grew faster due to enhanced treadmilling (Loisel et al., 1999) and reached lengths that exceeded 50 μm, indicating that under these conditions too they remain bound to FH1-FH2 for at least 1000 s.

mDia1 FH1-FH2 Enhances by 15-Fold the Rate Constant for Profilin-Actin Association to Barbed Ends

The rate of 0.4 μm/min (2.5 subunits/s) at which FH1-FH2 catalyzes barbed-end assembly in the presence of 0.1 μM profilin-actin is surprisingly high, considering the value of the rate constant for association of profilin-actin to barbed ends ($K_+ = 7$ μM$^{-1} \cdot$ s^{-1}; Gutsche-Perelroizen et al., 1999). To clarify this point, we monitored by fluorescence microscopy the initial rate of barbed-end growth of individual filaments using free, FH2 bound, or FH1-FH2 bound barbed ends (Figures 2A–2C). This method avoids the interference of mDia1-induced nucleation which, even at low-actin concentration, obscures its effect on K_+ in spectroscopic methods. The values of K_+ of G-actin or profilin-actin at the different classes of barbed ends were derived (Table 1). Free G-actin associated to FH2 or FH1-FH2 bound barbed ends 2-fold more slowly than to free barbed ends, in agreement with Li and Higgs (2003). Profilin-actin associated to free barbed ends slightly more slowly than G-actin, in agreement with Gutsche-Perelroizen et al. (1999). Profilin-actin associated to FH2 bound barbed ends 2-fold more slowly than to free barbed ends. In striking contrast, profilin-actin associated to FH1-FH2 bound barbed ends 15-fold faster than to free barbed ends. The value of K_+ of 110 μM$^{-1} \cdot$ s^{-1} at FH1-FH2 bound barbed ends overrides by 15-fold the diffusion-limited rate constant (Drenckhahn and Pollard, 1986). Thus, FH1-FH2 (but not FH2) acts as a motor steering barbed-end assembly of profilin-actin exclusively.

FH2 and FH1-FH2 also affect barbed-end disassembly. Both domains lowered by 2-fold the rate of depolymerization, consistent with their binding to barbed ends with equilibrium dissociation constants of 26 $\pm$ 8 nM for FH2 and 3 $\pm$ 1 nM for FH1-FH2 (Figure 2D). Since the value of K_+ for actin is lowered 2-fold by FH2 or FH1-FH2, the critical concentration ($Cc = K_-/K_+$) should not be affected by FH2 nor FH1-FH2. This implication

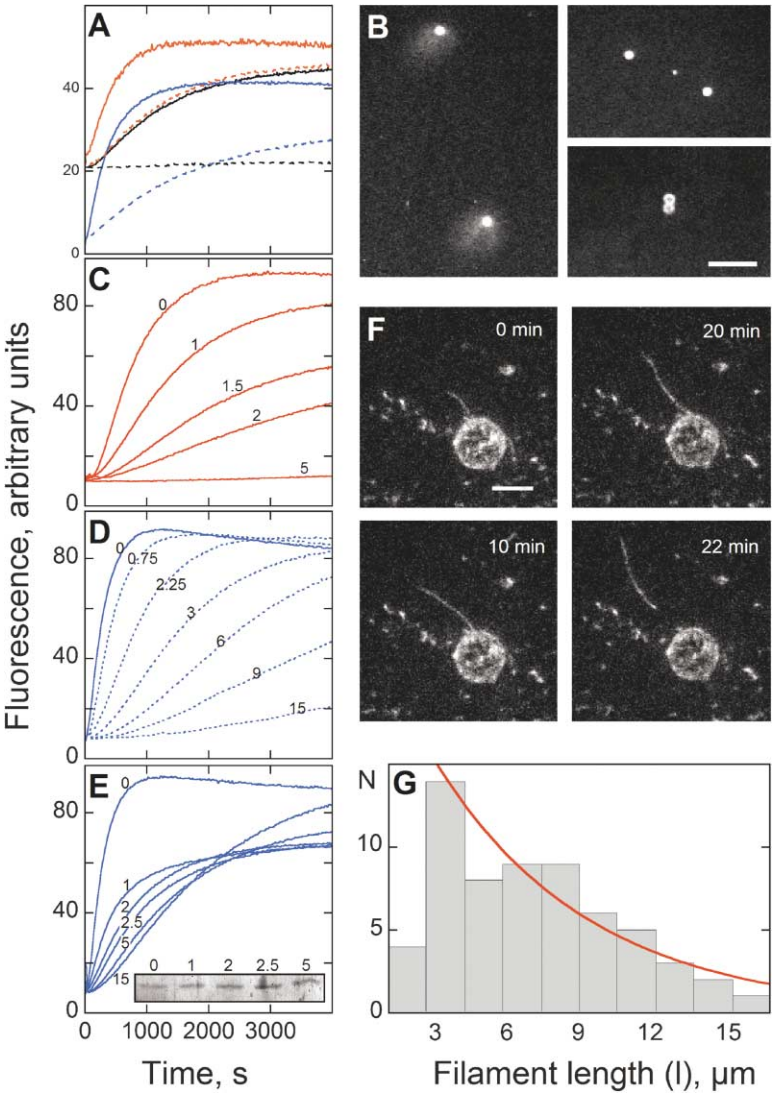

Figure 1. mDiaFH1-FH2 Catalyzes Site-Directed Processive Filament Assembly from Profilin-Actin and Remains Bound to Barbed Ends for 2000 s

(A) Actin (1.5 μM, 5% pyrenyl-labeled) was polymerized with BSA-coated beads (black curves) or with 13.5 pmol beads bound FH1-FH2 (red curves) or with 1.6 pmol soluble FH1-FH2 (blue curves) in a final volume of 160 μl, in the absence (continuous lines) or presence (dotted lines) of 5 μM profilin. The data show that 12% of beads bound FH1-FH2 is active.

(B) FH1-FH2-coated beads (2 μm in diameter) were removed from the polymerization assay (A) in the presence (left) and in the absence (top right) of profilin. Bottom right panel: FH2-coated beads with profilin. Filaments were stained with rhodamine-phalloidin. Bar = 10 μm.

(C) Profilin totally inhibits nucleation in the presence of FH2. Actin (1.5 μM, 5% pyrenyl-labeled) was polymerized in the presence of 40 nM FH2 and profilin (in μM).

(D) Ciboulot totally inhibits nucleation in the presence of FH1-FH2. Actin was polymerized as under (C) in the presence of 40 nM FH1-FH2 and ciboulot (in μM). Similar data are obtained with FH2.

(E) Profilin inhibits actin nucleation to a limited extent in the presence of FH1-FH2. Actin was polymerized as under (C) in the presence of 40 nM FH1-FH2 and profilin (in μM). Inset: SDS-gels of the supernatants of F-actin sedimented at the end of the polymerization process in the presence of profilin (in μM). An equal amount of actin is measured, showing that the lower fluorescence plateau at intermediate concentrations of profilin is an artifact (see Experimental Procedures).

(F) Timelapse recording of the processive growth of a single filament and its detachment from FH1-FH2-coated beads. Beads were placed in a solution of 0.5 μM rhodamine-F-actin, 4 μM profilin, and 0.15% methylcellulose and observed in fluorescence using an Ixon (Andor) electron-multiplying CCD back-illuminated camera. Bar: 5 μm.

(G) Histogram of the steady-state lengths reached by filaments from immobilized FH1-FH2. Conditions as under (F). The curve is the calculated exponential consistent with a detachment rate constant K_d of $7.5 \cdot 10^{-4}$ s^{-1}.

was verified (Supplemental Figure S2B on the *Cell* website). The value of K_+ for association of profilin-actin to barbed ends being greatly enhanced by FH1-FH2, the unchanged value of the critical concentration implies that the value of K_- should be enhanced by profilin to the same extent as K_+. This implication was verified (Figure 2E).

In conclusion, whereas FH1-FH2 processively assembles F-actin from profilin-actin, FH2 and FH1-FH2 work as leaky cappers in rapid equilibrium with barbed ends in the presence of pure actin (Zigmond et al., 2003).

The rate of barbed-end growth increased linearly with the concentration of profilin-actin, but slows down at high concentrations of profilin-actin, indicating that barbed-end growth is limited by a process slower than the on rate of profilin-actin. The extrapolated rate constant of this process derived from the model (Figure 6) was 60 s^{-1} for free barbed ends, in agreement with Gutsche-Perelroizen et al. (1999), and reached 340 s^{-1} for FH1-FH2 bound barbed ends.

mDia1 FH1-FH2 Increases the Rate of ATP Hydrolysis on Profilin-Actin at Barbed Ends and Uses It as a Source of Energy in Processive Filament Growth

Profilin binds at the barbed face of G-actin (Schutt et al., 1993). As filaments grow from profilin-actin, profilin must dissociate from the barbed end to restore a free barbed end available for further elongation. ATP hydrolysis on profilin bound actin lowers its affinity by 20-fold (Pantaloni and Carlier, 1993), allowing dissociation of profilin from the barbed end. Hence, ATP hydrolysis limits the rate of filament growth at high profilin-actin concentrations (Gutsche-Perelroizen et al., 1999). FH1-FH2 not only increases K_+ for profilin-actin but also promotes filament growth at rates that override the limit value of 60 s^{-1}. This fact suggests that ATP hydrolysis

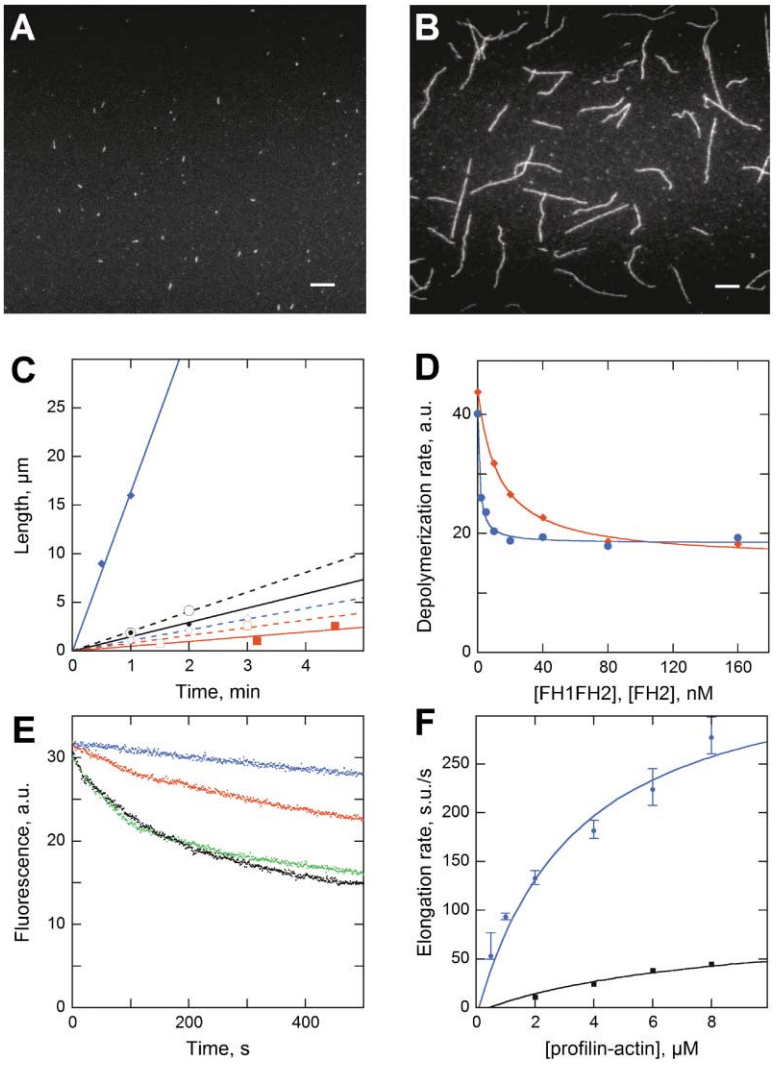

Figure 2. mDia1 FH1-FH2 Steers the Association of Profilin-Actin to Barbed Ends

Rhodamine-labeled actin (1.5 μM) was polymerized with 40 nM FH1-FH2 in the absence (A) and in the presence (B) of 5 μM profilin. Filaments formed at early time (60 s) of assembly, phalloidin-stabilized, were observed in TIRF microscopy. Bar = 5 μm.

(C) Initial rate of barbed-end growth from 1.5 μM actin, initiated by spectrin-actin seeds (black), FH2 (red), or FH1-FH2 (blue) and in the absence (dotted lines, open symbols) or in the presence (continuous lines, closed symbols) of 5 μM profilin. Symbols represent length measurements at the indicated times. The rate of growth is the slope of the lines.

(D) Formin slows down depolymerization of filaments at barbed ends. Dilution-induced depolymerization was measured in F buffer containing FH2 (red) or FH1-FH2 (blue). Curves are calculated using values of 3 nM and 26 nM for the equilibrium dissociation constants of FH1-FH2 and FH2 at barbed ends (equation in Experimental Procedures).

(E) Profilin increases the rate of depolymerization of FH1-FH2 bound barbed ends. F-actin (2 μM, 50% pyrenyl-labeled) was depolymerized by 50-fold dilution into F buffer containing 100 nM FH1-FH2 and profilin at 0 (blue), 10 (red), 25 (green), and 50 μM (black).

(F) Dependence of the rate of filament growth on profilin-actin concentration. Black: free barbed ends (spectrin-actin initiated growth). Blue: FH1-FH2 bound barbed ends. Measurements were made as in (C). The data points represent average lengths from the 20% longest filaments (see Experimental Procedures). Upper and lower bars represent average lengths calculated from the 15% and 25% longest filaments. Curves are calculated using the model (Figure 6) with the following values of rate constants: $K_1 = 110\ \mu M^{-1} \cdot s^{-1}$, $K_2 = 340\ s^{-1}$ for formin bound barbed ends and $K_1 = 7\ \mu M^{-1} \cdot s^{-1}$, $K_2 = 60\ s^{-1}$ for free barbed ends.

on profilin bound actin at the barbed end is accelerated by formin.

Hydrolysis of ATP is fast on MgATP-F-actin, making it difficult to detect a change in hydrolysis rate when assembly of profilin-MgATP-actin takes place at FH1-FH2 bound barbed ends. Hydrolysis is fast too on ATPγ-S-actin (M.-F.C, unpublished data). CaATP is hydrolyzed the most slowly on F-actin, in a manner largely uncoupled from polymerization (Carlier et al., 1986). Hence, profilin-CaATP-actin does not polymerize; profilin simply sequesters CaATP-actin (Perelroizen et al., 1996). A large uncoupling between polymerization and hydrolysis of ATP was also observed when polymerization of CaATP-actin was initiated by FH1-FH2 (Figure 3A). In contrast, FH1-FH2 induced fast polymerization of profilin-CaATP-actin with tight coupling of ATP hydrolysis (Figure 3B). Hence, ATP hydrolysis is accelerated on profilin-actin at FH1-FH2 bound barbed ends, thus allowing filaments to grow via consecutive rounds of profilin-actin association coupled to ATP hydrolysis

Table 1. Rate Constants for Actin and Profilin-Actin Association to Free, FH2 Bound, and FH1-FH2 Bound Barbed Ends

	Association Rate Constant to Barbed Ends, K_+ ($\mu M^{-1} \cdot s^{-1}$)		
Monomeric ATP-Actin Species	Free Barbed End	FH2 Bound Barbed End	FH1-FH2 Bound Barbed End
G-actin	9.5 (10)[a]	4	5.2
Profilin-actin	6.5 (7)[a]	2.5	110

The listed values of K_+ are derived from measurements carried out as under Figure 2C. The values given in parentheses refer to data coming from bulk measurements (fluorescence or turbidimetric measurements; Gutsche-Perelroizen et al., 1999).

[a] Gutsche-Perelroizen et al., 1999.

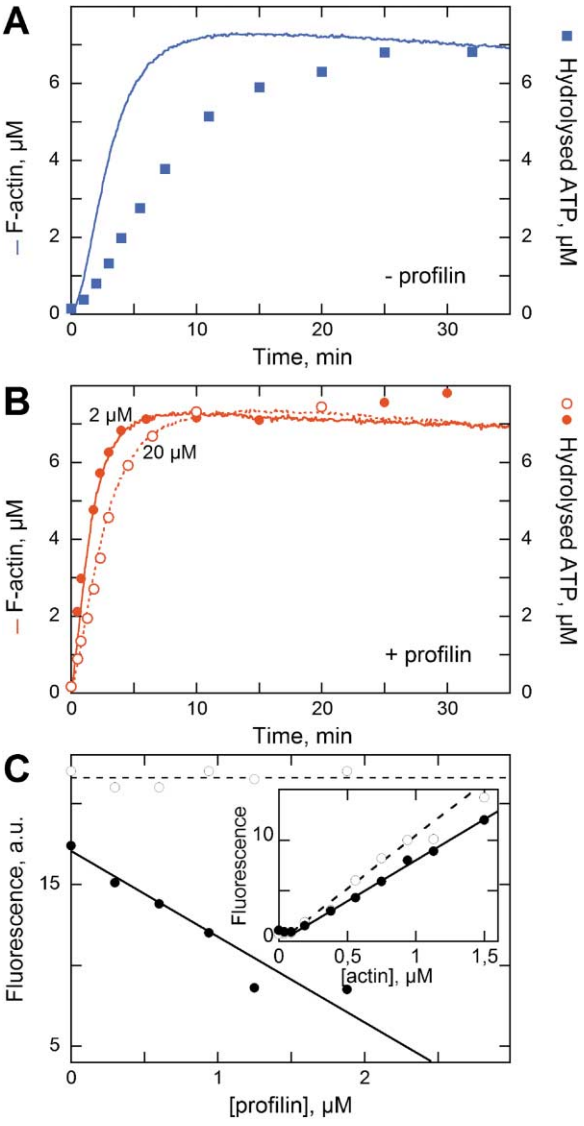

Figure 3. mDia1 FH1-FH2 Accelerates ATP Hydrolysis Associated with Profilin-Actin Assembly

Polymerization of γ-[^{32}P]-ATP-labeled CaATP-G-actin 1:1 complex (10 μM, containing 5% pyrenyl-actin) was initiated using 100 nM FH1-FH2. Lines: timecourses of polymerization monitored by pyrene fluorescence and converted in μM F-actin. Symbols: μM hydrolyzed ATP (acid-labile Pi).

(A) No profilin added. ATP hydrolysis occurs slowly on F-actin.

(B) Profilin was added at 2 μM (continuous line, closed circles) or 20 μM (dotted line, open circles). Note that at the substoichiometric amount of 2 μM profilin, tight coupling is observed between actin assembly and ATP hydrolysis, indicating that profilin is recycled in the consecutive rounds of assembly.

(C) In the presence of AMPPNP, profilin sequesters actin and does not allow processive filament growth at FH1-FH2 bound barbed ends. F-actin (2 μM, 2% pyrenyl-labeled), assembled in the presence of 120 nM FH1-FH2 in the presence of either ATP (open circles) or AMPPNP (closed circles) was supplemented with profilin. Inset: critical concentration plots in the presence of FH1-FH2 (125 nM), in ATP (open circles), and AMPPNP (closed circles). Note that fluorescence of AMPPNP-F-actin is 20% lower than that of ADP-F-actin.

(FH1-FH2 does not bind nor hydrolyze ATP, data not shown). Remarkably, formin and profilin act together to accelerate ATP hydrolysis by actin. Acceleration of MgATP hydrolysis on profilin-actin by FH1-FH2 likely accounts for the enhanced limiting rate of 340 s^{-1} for filament growth (Figure 2E).

In the presence of AMPPNP, actin polymerizes reversibly with identical critical concentrations (0.1 μM) at the two ends. FH1-FH2 nucleated assembly of AMPPNP-actin, but profilin did not support assembly of AMPPNP-actin at FH1-FH2 bound barbed ends (nor at free barbed ends) but promoted depolymerization of F-actin by sequestration (Figure 3C), as it does in ADP (Pantaloni and Carlier, 1993). Hence, formin-processive function requires ATP hydrolysis.

In conclusion, FH1-FH2-profilin-actin is a processive filament assembly machinery that accelerates hydrolysis of actin bound ATP at barbed ends, allowing the rapid release of profilin and subsequent filament assembly. The increase in K_+ above the diffusion-limited rate constant is another property of formin that adds up to its effect on ATP hydrolysis.

Insertional Profilin-Actin Polymerization at the Surface of FH1-FH2-Coated Beads Generates Actin-Based Propulsion

A biomimetic motility assay was designed to reconstitute controled formin-induced motility processes. FH2- or FH1-FH2-coated beads were placed in a solution of 7 μM rhodamine-labeled F-actin, 10 μM ADF/cofilin, and 3 μM profilin. This chemostat maintains a stationary amount of polymerizable G-actin via the rapid treadmilling of actin filaments (Didry et al., 1998). In the fluorescence microscope, FH1-FH2-coated beads initiated the formation of actin cables that spontaneously bundled in long actin tails. The propulsive force pushed the bead forward steadily at 10 μm/min (Figure 4A and Supplemental Movie S2 on the *Cell* website) for up to 2 hr. A laser-bleached zone of the actin tail moved away from the bead (kymograph in Figure 4B and Supplemental Movie S3 on the *Cell* website), consistent with FH1-FH2-driven processive insertional polymerization. In agreement with biochemical data, no bead movement was observed in solutions of only actin and ADF, nor when profilin was replaced by ciboulot. FH2-coated beads did not initiate an actin tail (data not shown). Hence, both profilin and FH1 are required for propulsion.

Motility assays confirmed the view that ATP hydrolysis is used in processive movement. First, hydrolysis of ATP into ADP by hexokinase and glucose or substitution of AMPPNP for ATP caused arrest of movement, while FH2 and FH1-FH2 do nucleate actin in ADP or AMPPNP. Finally, rapid movement of FH1-FH2-coated beads was observed as well with profilin-CaATP-actin as with profilin-MgATP-actin (data not shown).

In the presence of actin and 3 μM profilin but absence of ADF, movement was slow (0.4 μm/min). The velocity increased upon increasing ADF concentration and reached a plateau value of 15 μm/min (Figure 4C), consistent with the synergy between ADF and profilin (Didry et al., 1998). In the presence of actin and 10 μM ADF, no movement was observed, but velocity increased from 0 to 18 μm/min upon addition of increasing amounts of profilin (Figure 4D).

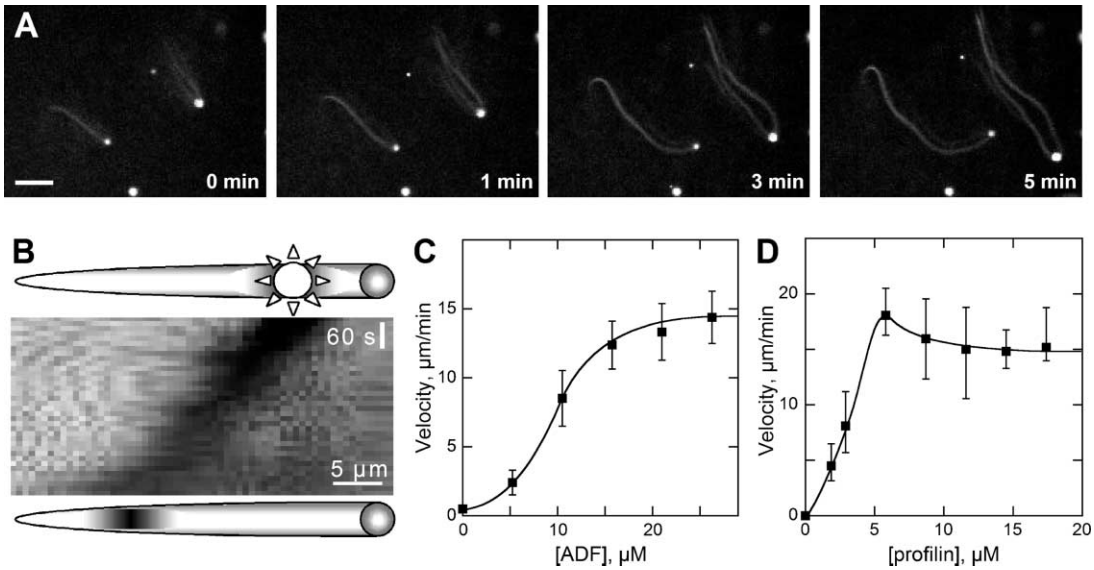

Figure 4. A Biomimetic Motility Assay Reconstitutes Rapid Formin-Induced Processes Observed In Vivo

(A) Timelapse recording of the propulsive movement of FH1-FH2-coated beads (2 μm in diameter) in the presence of 7 μM F-actin, 10 μM ADF, and 3 μM profilin. Bar = 10 μm.

(B) Kymograph of a bleached zone in the actin tail at the rear of an FH1-FH2-coated bead. Conditions: 7 μM F-actin, 5 μM ADF, 3 μM profilin. The laser flash is highlighted.

(C) ADF concentration dependence of the velocity of FH1-FH2-coated beads in a solution contatining 7 μM F-actin and 3 μM profilin. Note slow movement in the absence of ADF.

(D) Profilin concentration dependence of the velocity of FH1-FH2-coated beads in the presence of 7 μM F-actin and 10 μM ADF. No movement occurs in absence of profilin.

Capping Proteins Regulate the Rate and Duration of Profilin-Actin-Based Propulsion of FH1-FH2-Coated Beads

Since capping proteins are required for actin-based movement driven by WASP-Arp2/3 (Loisel et al., 1999), their effect on formin-associated motility was addressed. Addition of gelsolin or CapG to the motility medium containing actin, ADF, and profilin increased the rate of propulsion of FH1-FH2-coated beads. This effect is consistent with the increase in critical G-actin concentration due to the capping of barbed ends. Surprisingly, the increase in velocity was transient. After awhile, beads stopped; the actin tails detached from the beads that remained bare and never reinitiated actin assembly (Figure 5A and Supplemental Movies S4 and S5 on the *Cell* website). The velocity increased and the duration of the movement decreased upon increasing gelsolin concentration (Figure 5B). The fastest movement (30 μm/min, corresponding to 200 subunits assembled per second) was recorded for only 5 min in the presence of 7 μM actin, 100 nM gelsolin, 3 μM profilin, and 10 μM ADF. This speed is consistent with a steady-state amount of profilin-actin of 1.8 μM (200 s^{-1})/(110 $\mu M^{-1} \cdot s^{-1}$), which was verified by sedimentation (data not shown). When fresh beads were added to the solution following arrest of movement of a first batch of beads, they moved for the same period of time as the former ones and stopped. Immunodetection assays verified that formin was still bound to the beads. These data suggest that gelsolin gradually "poisons" the beads, preventing formin-catalyzed barbed-end growth by formation of an abortive complex with FH1-FH2, actin, and gelsolin.

Polymerization assays provide thermodynamic insight in the effect of capping proteins on formin-based motility. Capping proteins establish the high critical concentration of the pointed ends, while formins maintain the low critical concentration of the barbed ends (Li and Higgs, 2003; Pring et al., 2003; Supplemental Figure S3 on the *Cell* website). Formins have been reported to prevent the binding of capping proteins to barbed ends (Zigmond et al., 2003; Harris et al., 2004; Moseley et al., 2004). FH1-FH2 and cappers showed antagonistic competitive behavior in the control of the critical concentration (Figure 5C and Supplemental Figure S3 on the *Cell* website). Immunodetection assays showed that gelsolin was not displaced from pelleted filaments by FH1-FH2 (data not shown). In conclusion, FH1-FH2 shifts the F-actin steady state by creating new filaments with active barbed ends. The critical concentration is determined by the fraction of formin bound (active) and gelsolin bound (inactive) barbed ends.

CapG blocked the growth of free barbed ends (K_C = 0.8 nM), but blocked formin bound barbed ends with a higher value of K_C (60–70 nM), which remained constant in a large range of concentrations of FH1-FH2 or FH2 (Figure 5D). If formin and CapG were binding in direct competition, the value of K_C would increase linearly with the concentration of formin. In conclusion, CapG binds to formin bound barbed ends with a 100-fold lower affinity than to free barbed ends. Formation of the abortive complex of formin, actin, and gelsolin is likely responsible for the arrest of formin-based movements.

Discussion

We showed that the FH1-FH2 domain of mDia1 in complex with profilin-actin is a processive motor that drives

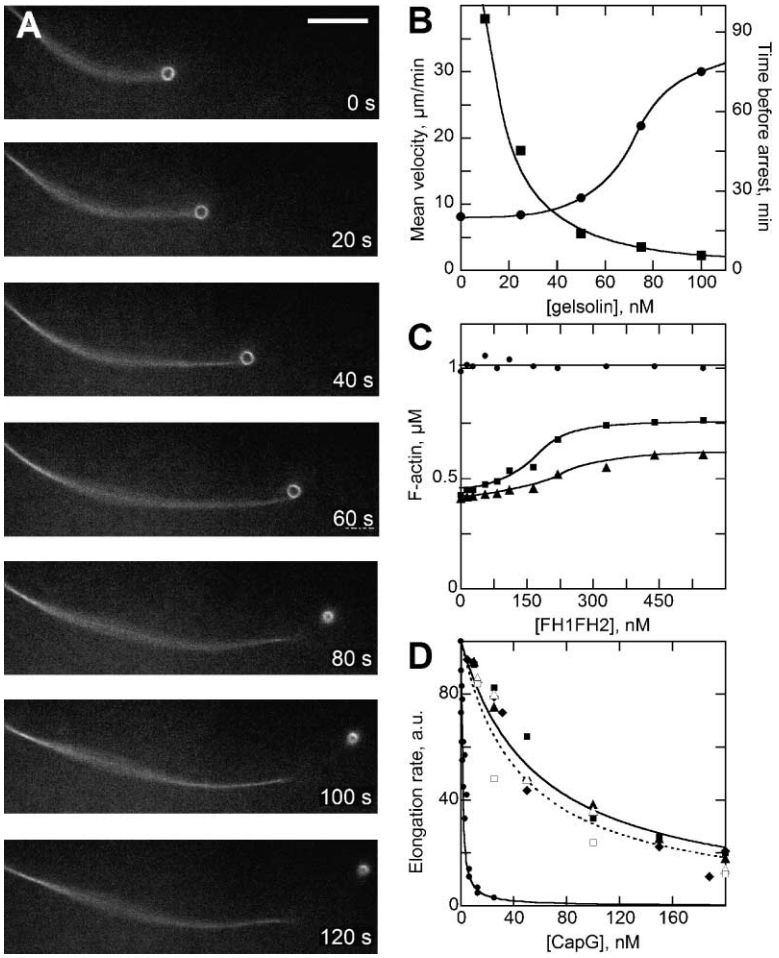

Figure 5. Capping Proteins Control the Activity of mDia1 in Actin Polymerization and in Motility

(A) Capping proteins arrest movement of formin-coated beads: timelapse recording of FH1-FH2-coated beads in a solution containing 10 μM actin, 10 μM ADF, 3 μM profilin, and 75 nM gelsolin. Bar = 10 μm.

(B) Gelsolin concentration dependence of the velocity (circles) and duration of movement (squares) of FH1-FH2-coated beads.

(C) Capping proteins and formin antagonize in the control of the steady state of actin assembly. F-actin (1.1 μM, 5% pyrenyl-labeled) was polymerized in the presence of CapG at 0 (circles), 100 (squares), and 200 nM (triangles) and supplemented with increasing amounts of FH1-FH2 as indicated. Fluorescence was recorded at steady state.

(D) Capping protein caps formin bound barbed ends with a 100-fold lower affinity than free barbed ends. The rate of initial barbed end growth was measured in spectrin-actin seeded growth assay (circles) or when barbed-end growth was initiated with 32 nM (closed triangles), 63 nM (closed diamonds), and 94 nM (closed squares) FH1-FH2 or 187 nM (open triangles) and 312 nM (open squares) FH2. Curves are calculated using K_c values of 0.8 nM for CapG binding to free barbed ends and 55 nM and 45 nM for CapG binding to FH1-FH2 and FH2 barbed ends, respectively.

rapid barbed-end assembly of several micrometer-long actin filaments for periods up to 2000 s. The motor has the following features: first, the rate constant for profilin-actin association to barbed ends, K_+, is increased by 15-fold, up to 110 $\mu M^{-1} \cdot s^{-1}$, by formin. This property accounts for the rapid (up to 0.29 μm/s) sustained movement of formin-coated beads in a biomimetic assay containing actin, ADF, and profilin. Second, formin-induced increase in K_+ is linked to a large acceleration of ATP hydrolysis coupled to profilin-actin assembly, thus allowing growth rates of up to 340 subunits/s. Finally, the rate and duration of formin-based motile processes are regulated by capping proteins.

Molecular Mechanism for Processive Filament Assembly from Profilin-Actin by mDia1

FH2-actin and FH1-profilin interactions are required for the processivity of the FH1-FH2 domain in barbed-end assembly. In the absence of profilin, FH2 as well as FH1-FH2 nucleate actin filaments and bind to barbed ends as leaky cappers in rapid equilibrium, slowing down 2-fold G-actin association-dissociation at barbed ends. FH1-FH2-coated beads do not move in a solution of actin and ADF only, which yet supports rapid treadmilling.

Profilin causes a dramatic change in FH1-FH2 properties. The barbed-end bound FH1-FH2-profilin-actin complex is a unique processive machinery that accelerates elongation, thus overriding the diffusion limit by a steering effect that may have an electrostatic or hydrodynamic origin (Frisch et al., 2001; Brune and Kim, 1994). A solution of F-actin, ADF, and profilin supports the steady movement of formin-coated particles with the same characteristics of rapid growth (0.29 μm/s) as actin cables in yeast (Yang and Pon, 2002), E-GFP-tagged mDia1ΔN3 speckles in XTC fibroblasts (Higashida et al., 2004), and other rapid actin-based processes such as assembly of the cytokinetic ring (Arai and Mabuchi, 2002) and possibly extension of filopodia (Peng et al., 2003). So far, such processes were thought to require very high cellular concentrations of polymerizable G-actin. The processes are actually observed in a solution that maintains a steady concentration of only 1–2 μM profilin-actin, close to plausible physiological values. Thus, under physiological conditions, actin-based processes are powered simultaneously at different velocities in the cell by N-WASP-Arp2/3 (2 μm/min) or formin (15 μm/min). mDia1 remains attached to a growing end up to 2000 s, allowing growth of 7–10 μm-long filaments at steady state in the absence of ADF, and much longer (50 μm or more) in the presence of ADF. The function of profilin in mDia1-based movement is not restricted to its sole effect on treadmilling, unlike in N-WASP-Arp2/3 motility.

A source of free energy is required for processivity. Formin is the first regulatory protein that accelerates ATP hydrolysis on profilin-actin and uses the released

free energy for its processive function. How profilin and formin cooperate in enhancing ATP hydrolysis, as a "GAP" does on small G proteins, is an important structural issue raised by these findings. The environment of the ATP binding site in the formin-profilin-actin complex must be modified. The associated conformational changes in this complex affect the electrostatic or hydrodynamic nature of the barbed end, allowing a local steering of profilin-actin association. Faster ATP hydrolysis is not formally required for the increased value of K_+ but may be a contingent property linked to this other effect of formin. The rate of formin-catalyzed filament assembly is limited to 340 s^{-1} at high profilin-actin concentrations. This value represents either the rate of ATP hydrolysis or of subsequent Pi release or of dissociation of profilin from barbed-end bound actin. Yet, ATP hydrolysis must occur at least at 340 s^{-1}.

Our data provide a rationale to genetic studies showing the requirement of profilin in the assembly of the cytokinetic ring (Severson et al., 2002) and actin cables (Evangelista et al., 2002). Slow formin-associated processes observed upon transfection of cells with a nonprocessive FH2 domain of mDia1 (Copeland and Treisman, 2002; Higashida et al., 2004) may be due to formation of poorly processive dimers of FH2 with the endogenous active mDia1.

Model for Catalysis of Processive Barbed-End Growth by the Formin-Profilin-Actin Machinery

Formin remains bound to the barbed end for many consecutive cycles of profilin-actin assembly. In the absence of profilin, FH1-FH2 is in rapid equilibrium with a barbed end; hence, rapid dissociation of FH1-FH2 from a barbed end is expected to occur following ATP hydrolysis and dissociation of profilin from actin. To obtain a processive action, though, cycles of attachment-detachment of the same formin must mediate its stepping walk along the terminal F-actin subunits as the filament grows. The dimeric structure of FH1-FH2 (Xu et al., 2004) solves this paradox. A model describing the processive walk of formin at barbed ends is proposed based on structural and present biochemical data (Figure 6). Processive assembly results from a cycle in which each of the FH1-FH2 protomers alternately binds the terminal profilin-ATP-F-actin and dissociates from subterminal ADP-F-actin following release of profilin. We propose that ATP hydrolysis on the actin subterminal subunit, coupled to the lateral actin-actin contact with the terminal profilin-actin subunit, is the source of energy for the processive walk of formin. An analytical expression of the rate of filament elongation has been derived for this type of model (Pantaloni et al., 1985). A similar clamped-filament elongation model has been proposed for actin-based motors (Dickinson and Purich, 2002). Our model accounts for nucleation of filaments from formin-profilin-actin: enhancing ATP hydrolysis leads to dissociation of profilin from a profilin-actin lateral dimer and allows trimer formation.

Filament growth generates a 5 nm pitch left-handed helix. When filaments grow from immobilized formin, either the filament rotates 167°/subunit around its axis as it grows from surface bound formin or the two FH1-FH2 protomers of the formin dimer undergo an oscillating torque motion to accommodate filament straight growth. The former mechanism seems unlikely and was dismissed by the fact that actin-based propulsion of formin-coated beads was not altered by addition of α-actinin, which prevents the free rotation of individual filaments by bridging them (data not shown). In the latter mechanism, the flexibility of the formin dimer, suggested by the flexible tether in the FH2 dimer (Xu et al., 2004), plays a role in the motor function of formin. Yet the FH2 domain has no processive function. Some additional features in FH1-FH2 may generate internal motions in formin. Structural studies of the complexes of formin with actin and profilin should elucidate the structural basis for the motor function.

Interplay between Capping Proteins and Formins in the Control of Barbed-End Growth

Capping proteins are required for efficient N-WASP-mediated processes, maintained by a balance between the creation of new filaments by branching and the death of the filaments by capping. Formin-based motility is more sensitive to capping proteins since formins do not generate filaments autocatalytically. Factors that affect the lifetime of formin at filament ends are expected to regulate movement. We confirm (Zigmond et al., 2003) that mDia1 lowers the affinity of capping proteins for barbed ends by 100-fold; however, mDia1 and capping proteins do not bind in direct competition. Capping proteins may bind to a formin bound filament at an intermediate step of the processive cycle, in an abortive complex that arrests the movement of formin-coated beads. In vivo, cytochalasin D, which caps barbed ends, arrested formin-induced movement (Higashida et al., 2004). Capping proteins may promote the observed release of bundles from bud sites (Yang and Pon, 2002). This timer function generated by the characteristics of the processive cycle may as well control formin-dependent processes such as the assembly and disassembly of the cytokinetic ring.

Force Generation by Site-Directed Processive Polymerization of Unbranched Filaments

Growth of actin filaments generates a propulsive force of 3.5 pN/filament, assuming 2 μM polymerizable actin (Mogilner and Oster, 1996). Like in N-WASP-Arp2/3-mediated actin-based movement (Theriot et al., 1992), the rate of propulsion of formin-coated beads equals the rate of polymerization, although the detailed molecular mechanisms are different. The bundled filaments generated by formin must have mechanical and rheological properties different from the entangled gel generated by Arp2/3-branched filaments. The role played by the elasticity of the actin gel in motility processes can now be addressed by measuring the forces that are produced by the two systems operating in identical synthetic chemically controlled media.

Experimental Procedures

Proteins

Actin was purified and pyrenyl- or rhodamine-labeled (Carlier et al., 1986; Isambert et al., 1995). Recombinant FH2 (752–1194) and FH1-FH2-COOH (569–1255) domains of mDia1 were expressed as His-tagged fusion proteins in *E. coli* BL21. Bacteria were grown at 37°C

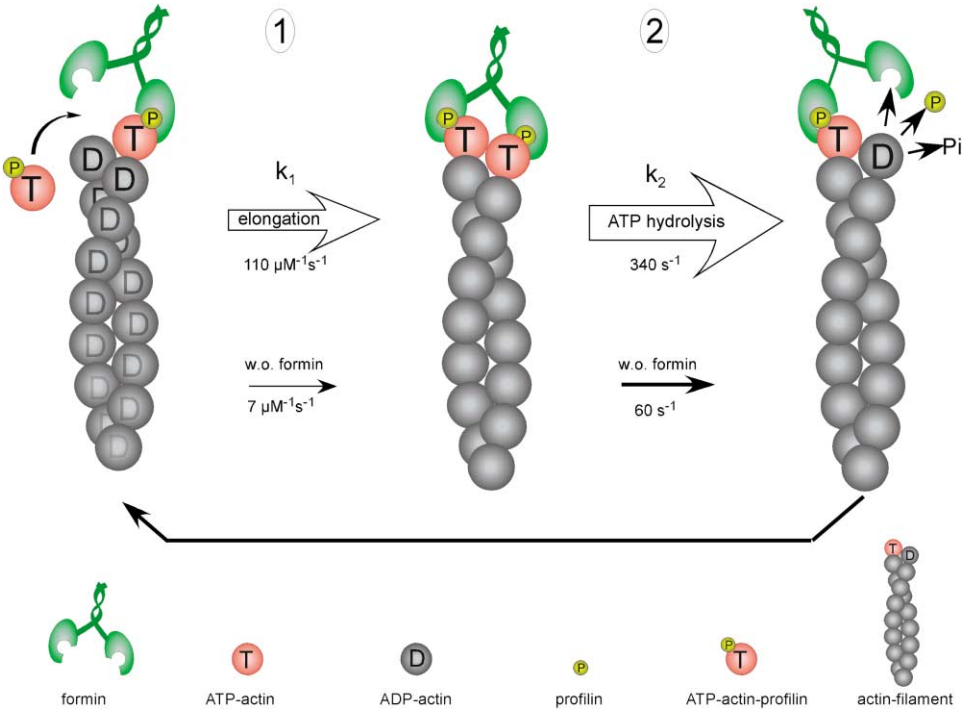

Figure 6. Model for the Processive Action of Formin in Barbed-End Assembly of Profilin-Actin

Processive steady barbed-end growth is described by a two-step cycle. In the first step (bimolecular rate constant K_1), profilin-actin associates to a barbed end to which formin and profilin-ATP-actin are bound. Profilin (P) interacts with the FH1 domain, while the FH2 domain interacts with the terminal ATP-F-actin subunit (A). The resulting barbed end has terminal and subterminal PA subunits. Each PA interacts with one FH1-FH2 subunit of the dimer. The second step accounts for the hydrolysis of ATP, release of Pi, and subsequent release of profilin from the subterminal actin subunit. A single rate constant K_2 represents the slowest of these three consecutive processes. In the steady-state cycle, all rates are equal. At low profilin-actin concentration, the slowest step that controls the cycle is step 1; at higher concentration of profilin-actin, step 2 (ATP hydrolysis or release of profilin) controls the cycle, causing the curvature of the plot (Figure 4E).
The structure of FH1-FH2 being unknown, the drawn shape of the protein is illustrative and has no structural significance.

to log phase, induced with 1 mM IPTG and grown for 16 hr at 16°C. Cells were pelleted, washed, resuspended in 20 mM phosphate, 20 mM imidazole (pH 7.8)/0.5 M KCl/10 mM MgCl with protease inhibitors, and lysed by sonication. The lysate, cleared by centrifugation at 17,000 × g, was incubated with NiNTA agarose beads (Qiagen). Following a wash with 50 mM imidazole, His-tagged proteins were eluted with 250 mM imidazole, dialyzed against 100 mM Tris (pH 7.5)/0.1 M KCl/1 mM DTT, centrifuged at 400,000 × g, and flash-frozen in liquid nitrogen. No change in activity was recorded upon freezing the proteins nor upon removing the His-tag. Recombinant human gelsolin and CapG were given by A. Zapun. Human ADF and ciboulot were expressed in *E. coli* (Hertzog et al., 2004). Profilin was purified from bovine spleen (Pantaloni and Carlier, 1993).

Actin Polymerization Assays

Actin polymerization was monitored in 5 mM Tris (pH 7.6), 0.2 mM ATP, 0.1 mM $CaCl_2$, 1 mM DTT, 1 mM $MgCl_2$, 0.1 M KCl, and 0.2 mM EGTA. EGTA and $MgCl_2$ were omitted in polymerization of CaATP-actin. The increase in fluorescence of 1% to 5% pyrenyl-labeled actin was monitored using a Safas spectrofluorimeter (λ_{exc} = 366 nm, λ_{em} = 407 nm). When actin was assembled in the presence of FH1-FH2 and profilin, a lower fluorescence plateau was reached in a range of intermediate concentrations of profilin. The fluorescence increased to the same value as in other samples in 18 hr. Sedimentation assays showed that the low fluorescence does not correspond to a lower amount of polymerized actin but results from the lower affinity of profilin for pyrenyl-labeled than for unlabeled actin and from the fact that in processive filament assembly from profilin-actin, long stretches of consecutive poorly labeled F-actin subunits are incorporated. This effect became fainter at high profilin, allowing the profilin's binding to pyrenyl-actin, and vanished upon overnight incubation due to the turnover of filaments and redistribution of labeled actin.

Dilution-induced depolymerization of F-actin was monitored following 50-fold dilution of a 2 μM F-actin (50% pyrenyl-labeled) solution in F buffer containing formin at different concentrations. The initial rate of depolymerization was analyzed using the equation $V = V_0 - ([V_0 - V_{min}]/[1 + K_d/(F)])$, where V, V_0, and V_{min} are the rates measured in the presence of formin at concentration (F), in the absence of formin, and at saturation by formin, and K_d is the equilibrium dissociation constant of the complex of formin with a filament barbed end.

Steady-state pyrene fluorescence measurements of F-actin assembly were carried out in a Spex spectrofluorimeter following overnight incubation of samples at 4°C.

Characterization of mDia1-Coated Beads

Carboxylated polystyrene microspheres (2 μm, Polyscience, 0.25% solids suspension) were incubated with FH1-FH2 or FH2 (10 μM for standard beads, 0.5 μM for poorly coated beads) in Xb-buffer (10 mM HEPES [pH 7.8], 0.1 M KCl, 1 mM $MgCl_2$, 1 mM ATP, and 0.1 mM $CaCl_2$) for 1 hr, washed and saturated with 1% BSA, and stored in 0.1% BSA.

The amount of FH1-FH2 or FH2 immobilized on the beads was determined by SDS-PAGE (Wiesner et al., 2003). Surface densities of 0.10 FH1-FH2 molecule/nm^2 and 0.06 FH2 molecule/nm^2 were obtained, corresponding to almost close packing distances of 3 nm and 4 nm between FH1-FH2 and FH2.

Motility Assay with mDia1-Coated Beads

The standard motility medium consisted of 7 μM F-actin (16% rhodamine-labeled) in Xb-buffer, 10 μM ADF/cofilin, 3 μM profilin, 1%

BSA, 0.2% (wt/vol) methyl cellulose (cat. # M-0512 Sigma-Aldrich), 7 mM DTT, and 1.5 mM diazo-bicyclo-octane (DABCO). Changes in the composition of this medium are indicated. Average rates of movement were determined by synchronous recording of four selected fields (CCD camera Orca II ERG, Hamamatsu) using an Olympus AX70 microscope and MetaMorph 5.0 software (Universal Imaging Corp.) for microscope control and image acquisition. A 20× (NA 0.5) or a 100× phase objective (NA 1.35) was used. Freely moving beads from at least ten different fields were selected. The template recognition-based tracking tool or the kymograph tool of MetaMorph was used to measure mean velocities, calculated for sets of 10–15 beads.

Fluorescence Microscopy Measurements of the Rate of Growth of Individual Filaments

Polymerization of actin (2% pyrenyl-labeled, 98% rhodamine-labeled) in absence or presence of profilin was initiated either from spectrin-actin or from formin. In control assays, the kinetic parameters for actin assembly were unaffected by rhodamine labeling. Aliquots were removed from the solution at early times of assembly (less than 60 s in the presence of profilin), monitored by pyrene fluorescence, when less than 5% of G-actin had assembled in filaments. Filaments were immediately diluted 100-fold in F buffer containing 5 μM phalloidin and processed for observation in TIRF microscopy. This method uniquely allows appropriate initial rate measurements at early times and was preferred to real-time TIRF monitoring of filament growth that provides biased data due to a dead time greater than 1 min. Histograms of length distribution were recorded from images of at least 1000 filaments for each time point, using MetaMorph software. This assay is selective for the effect of profilin on elongation, in contrast to spectroscopically monitored nucleation growth (Sagot et al., 2002b; Li and Higgs, 2003; Figure 1E). To eliminate the artifact in the measurements arising from the continuous nucleation by formin in the investigated time interval, only the 20% longest filaments, which had nucleated very early, were considered in the length versus time measurements. Different concentrations of profilin-actin were obtained by adding profilin to G-actin in a proportion of one molar equivalent + 5 μM. The possibility that reannealing of filaments biased the interpretation of the data was ruled out as follows: parallel samples polymerizing with 10% Alexa488-labeled actin and rhodamine-labeled actin were mixed at different early time intervals and observed in initial rate conditions as above. No double labeling of the filaments was detected, testifying that no reannealing took place. The values of the association rate constant of G-actin or profilin-actin to free or formin bound barbed ends, K_+, were derived from the initial rate of filament growth, V_e, (in subunits/s) using the equation $V_e = K_+ \cdot (C - Cc)$, where Cc is the critical concentration at barbed ends. The values found for K_+ of G-actin and profilin-actin at the free barbed ends were in quantitative agreement with those derived from bulk fluorescence or turbidimetric measurements, thus validating the method.

To evaluate the average time period for which FH1-FH2 remains bound to a growing end, coated beads were placed in 0.5 μM rhodamine-labeled F-actin + 4 μM profilin at time zero. The average length of attached filaments increased and reached a stationary value, reflecting an established balance between the continuous nucleation of filaments that grow in the attached state at a constant rate $K_+ \cdot (C - Cc)$ and the detachment of these filaments with a rate constant K_d. A histogram of the stationary length distribution N(l) was built. The value of K_d was derived from the exponential decline in N versus l.

ATP Hydrolysis Associated with Actin Polymerization

G-actin bound ATP was labeled γ-[^{32}P]-ATP. The γ-[^{32}P]-ATP-G-actin 1:1 complex was isolated by treatment with Dowex-1. Cleavage of ATP during polymerization was measured at time intervals as described (Carlier et al., 1986).

Modeling of Formin-Catalyzed Processive Actin Polymerization

The Berkeley-Madonna software was used, with the following equations, to model formin function in actin assembly:

$$F^* - PA + PA \rightarrow F^* - (PA)_2 \quad (1)$$

$$F^* - (PA)_2 \rightarrow F^* - PA + P + Pi \quad (2)$$

$$F^* - PA + P \rightarrow F^* - PA + PA \quad (3)$$

Equation 1 describes association (rate constant K_1) of profilin-actin (PA) to a filament barbed end that has formin FH1-FH2 bound in association with PA as terminal subunit (F*-PA). Equation 2 describes the hydrolysis of ATP and dissociation of inorganic phosphate (Pi) and profilin (P) from the subterminal position. Equation 3 is required to account for establishment of a steady state.

Acknowledgments

mDia1 cDNA was kindly provided by Dr. Shuh Narumiya (Kyoto University Faculty of Medicine). We are grateful to Drs. Rong Li and Maud Hertzog for helpful comments on the manuscript and critical reading. We thank Olivier Bernard (Andor Technology) for lending the IXON camera for ultrasensitive dynamic digital imaging (Figure 1F). This work was supported in part by the Ligue Nationale contre le Cancer to M.-F.C. (équipe labellisée) and by an HFSP grant # RGP72/2003 to M.-F.C. C.E. is supported by a Human Frontier Science Postdoctoral Fellowship (LT00029/2000-M). S.R. is supported by a predoctoral training fellowship from the French Ministry of Research.

Received: April 30, 2004
Revised: September 3, 2004
Accepted: September 13, 2004
Published: October 28, 2004

References

Alberts, A.S. (2001). Identification of a carboxyl-terminal diaphanous-related formin homology protein autoregulatory domain. J. Biol. Chem. *276*, 2824–2830.

Arai, R., and Mabuchi, I. (2002). F-actin ring formation and the role of F-actin cables in the fission yeast Schizosaccharomyces pombe. J. Cell Sci. *115*, 887–898.

Boquet, I., Boujemaa, R., Carlier, M.F., and Preat, T. (2000). Ciboulot regulates actin assembly during *Drosophila* brain metamorphosis. Cell *102*, 797–808.

Brune, D., and Kim, S. (1994). Hydrodynamic steering effects in protein association. Proc. Natl. Acad. Sci. USA *91*, 2930–2934.

Carlier, M.F., Pantaloni, D., and Korn, E.D. (1986). The effects of Mg2+ at the high-affinity and low-affinity sites on the polymerization of actin and associated ATP hydrolysis. J. Biol. Chem. *261*, 10785–10792.

Copeland, J.W., and Treisman, R. (2002). The diaphanous-related formin mDia1 controls serum response factor activity through its effects on actin polymerization. Mol. Biol. Cell *13*, 4088–4099.

Dickinson, R.B., and Purich, D.L. (2002). Clamped-filament elongation model for actin-based motors. Biophys. J. *82*, 605–617.

Didry, D., Carlier, M.F., and Pantaloni, D. (1998). Synergy between actin depolymerizing factor/cofilin and profilin in increasing actin filament turnover. J. Biol. Chem. *273*, 25602–25611.

Dong, Y., Pruyne, D., and Bretscher, A. (2003). Formin-dependent actin assembly is regulated by distinct modes of Rho signaling in yeast. J. Cell Biol. *161*, 1081–1092.

Drenckhahn, D., and Pollard, T.D. (1986). Elongation of actin filaments is a diffusion-limited reaction at the barbed end and is accelerated by inert macromolecules. J. Biol. Chem. *261*, 12754–12758.

Evangelista, M., Blundell, K., Longtine, M.S., Chow, C.J., Adames, N., Pringle, J.R., Peter, M., and Boone, C. (1997). Bni1p, a yeast formin linking cdc42p and the actin cytoskeleton during polarized morphogenesis. Science *276*, 118–122.

Evangelista, M., Pruyne, D., Amberg, D.C., Boone, C., and Bretscher, A. (2002). Formins direct Arp2/3-independent actin filament assembly to polarize cell growth in yeast. Nat. Cell Biol. *4*, 260–269.

Evangelista, M., Zigmond, S., and Boone, C. (2003). Formins: signaling effectors for assembly and polarization of actin filaments. J. Cell Sci. *116*, 2603–2611.

Frisch, C., Fersht, A.R., and Schreiber, G. (2001). Experimental assignment of the structure of the transition state for the association of barnase and barstar. J. Mol. Biol. *308*, 69–77.

Gasman, S., Kalaidzidis, Y., and Zerial, M. (2003). RhoD regulates endosome dynamics through Diaphanous-related Formin and Src tyrosine kinase. Nat. Cell Biol. *5*, 195–204.

Gutsche-Perelroizen, I., Lepault, J., Ott, A., and Carlier, M.F. (1999). Filament assembly from profilin-actin. J. Biol. Chem. *274*, 6234–6243.

Harris, E.S., Li, F., and Higgs, H.N. (2004). The mouse formin, FRLalpha, slows actin filament barbed end elongation, competes with capping protein, accelerates polymerization from monomers, and severs filaments. J. Biol. Chem. *279*, 20076–20087.

Hertzog, M., van Heijenoort, C., Didry, D., Gaudier, M., Coutant, J., Gigant, B., Didelot, G., Préat, T., Knossow, M., Guittet, E., and Carlier, M.F. (2004). The β-thymosin/WH2 domain: Structural basis for the switch from inhibition to promotion of assembly. Cell *117*, 611–623.

Higashida, C., Miyoshi, T., Fujita, A., Oceguera-Yanez, F., Monypenny, J., Andou, Y., Narumiya, S., and Watanabe, N. (2004). Actin polymerization-driven molecular movement of mDia1 in living cells. Science *303*, 2007–2010.

Isambert, H., Venier, P., Maggs, A.C., Fattoum, A., Kassab, R., Pantaloni, D., and Carlier, M.F. (1995). Flexibility of actin filaments derived from thermal fluctuations. Effect of bound nucleotide, phalloidin, and muscle regulatory proteins. J. Biol. Chem. *270*, 11437–11444.

Kato, T., Watanabe, N., Morishima, Y., Fujita, A., Ishizaki, T., and Narumiya, S. (2001). Localization of a mammalian homolog of diaphanous, mDia1, to the mitotic spindle in HeLa cells. J. Cell Sci. *114*, 775–784.

Kobielak, A., Pasolli, H.A., and Fuchs, E. (2004). Mammalian formin-1 participates in adherens junctions and polymerization of linear actin cables. Nat. Cell Biol. *6*, 21–30.

Koka, S., Neudauer, C.L., Li, X., Lewis, R.E., McCarthy, J.B., and Westendorf, J.J. (2003). The formin-homology-domain-containing protein FHOD1 enhances cell migration. J. Cell Sci. *116*, 1745–1755.

Kovar, D.R., Kuhn, J.R., Tichy, A.L., and Pollard, T.D. (2003). The fission yeast cytokinesis formin Cdc12p is a barbed end actin filament capping protein gated by profilin. J. Cell Biol. *161*, 875–887.

Lee, L., Klee, S.K., Evangelista, M., Boone, C., and Pellman, D. (1999). Control of mitotic spindle position by the Saccharomyces cerevisiae formin Bni1p. J. Cell Biol. *144*, 947–961.

Li, F., and Higgs, H.N. (2003). The mouse Formin mDia1 is a potent actin nucleation factor regulated by autoinhibition. Curr. Biol. *13*, 1335–1340.

Loisel, T.P., Boujemaa, R., Pantaloni, D., and Carlier, M.F. (1999). Reconstitution of actin-based motility of Listeria and Shigella using pure proteins. Nature *401*, 613–616.

Machesky, L.M., and Insall, R.H. (1998). Scar1 and the related Wiskott-Aldrich syndrome protein, WASP, regulate the actin cytoskeleton through the Arp2/3 complex. Curr. Biol. *8*, 1347–1356.

Mogilner, A., and Oster, G. (1996). Cell motility driven by actin polymerization. Biophys. J. *71*, 3030–3045.

Moseley, J.B., Sagot, I., Manning, A.L., Xu, Y., Eck, M.J., Pellman, D., and Goode, B.L. (2004). A conserved mechanism for Bni1- and mDia1-induced actin assembly and dual regulation of Bni1 by Bud6 and profilin. Mol. Biol. Cell *15*, 896–907.

Ozaki-Kuroda, K., Yamamoto, Y., Nohara, H., Kinoshita, M., Fujiwara, T., Irie, K., and Takai, Y. (2001). Dynamic localization and function of Bni1p at the sites of directed growth in Saccharomyces cerevisiae. Mol. Cell. Biol. *21*, 827–839.

Pantaloni, D., and Carlier, M.F. (1993). How profilin promotes actin filament assembly in the presence of thymosin beta 4. Cell *75*, 1007–1014.

Pantaloni, D., Hill, T.L., Carlier, M.F., and Korn, E.D. (1985). A model for actin polymerization and the kinetic effects of ATP hydrolysis. Proc. Natl. Acad. Sci. USA *82*, 7207–7211.

Pelham, R.J., and Chang, F. (2002). Actin dynamics in the contractile ring during cytokinesis in fission yeast. Nature *419*, 82–86.

Peng, J., Wallar, B.J., Flanders, A., Swiatek, P.J., and Alberts, A.S. (2003). Disruption of the Diaphanous-related formin Drf1 gene encoding mDia1 reveals a role for Drf3 as an effector for Cdc42. Curr. Biol. *13*, 534–545.

Perelroizen, I., Didry, D., Christensen, H., Chua, N.H., and Carlier, M.F. (1996). Role of nucleotide exchange and hydrolysis in the function of profilin in action assembly. J. Biol. Chem. *271*, 12302–12309.

Pollard, T.D., and Cooper, J.A. (1984). Quantitative analysis of the effect of Acanthamoeba profilin on actin filament nucleation and elongation. Biochemistry *23*, 6631–6641.

Pring, M., Evangelista, M., Boone, C., Yang, C., and Zigmond, S.H. (2003). Mechanism of formin-induced nucleation of actin filaments. Biochemistry *42*, 486–496.

Pruyne, D., Evangelista, M., Yang, C., Bi, E., Zigmond, S., Bretscher, A., and Boone, C. (2002). Role of formins in actin assembly: nucleation and barbed-end association. Science *297*, 612–615.

Riveline, D., Zamir, E., Balaban, N.Q., Schwarz, U.S., Ishizaki, T., Narumiya, S., Kam, Z., Geiger, B., and Bershadsky, A.D. (2001). Focal contacts as mechanosensors: externally applied local mechanical force induces growth of focal contacts by an mDia1-dependent and ROCK-independent mechanism. J. Cell Biol. *153*, 1175–1186.

Sagot, I., Klee, S.K., and Pellman, D. (2002a). Yeast formins regulate cell polarity by controlling the assembly of actin cables. Nat. Cell Biol. *4*, 42–50.

Sagot, I., Rodal, A.A., Moseley, J., Goode, B.L., and Pellman, D. (2002b). An actin nucleation mechanism mediated by Bni1 and profilin. Nat. Cell Biol. *4*, 626–631.

Schutt, C.E., Myslik, J.C., Rozycki, M.D., Goonesekere, N.C., and Lindberg, U. (1993). The structure of crystalline profilin-beta-actin. Nature *365*, 810–816.

Severson, A.F., Baillie, D.L., and Bowerman, B. (2002). A Formin Homology protein and a profilin are required for cytokinesis and Arp2/3-independent assembly of cortical microfilaments in *C. elegans*. Curr. Biol. *12*, 2066–2075.

Shimada, A., Nyitrai, M., Vetter, I.R., Kuhlmann, D., Bugyi, B., Narumiya, S., Geeves, M.A., and Wittinghofer, A. (2004). The core FH2 domain of diaphanous-related formins is an elongated actin binding protein that inhibits polymerization. Mol. Cell *13*, 511–522.

Theriot, J.A., Mitchison, T.J., Tilney, L.G., and Portnoy, D.A. (1992). The rate of actin-based motility of intracellular Listeria monocytogenes equals the rate of actin polymerization. Nature *357*, 257–260.

Tolliday, N., VerPlank, L., and Li, R. (2002). Rho1 directs formin-mediated actin ring assembly during budding yeast cytokinesis. Curr. Biol. *12*, 1864–1870.

Tominaga, T., Sahai, E., Chardin, P., McCormick, F., Courtneidge, S.A., and Alberts, A.S. (2000). Diaphanous-related formins bridge Rho GTPase and Src tyrosine kinase signaling. Mol. Cell *5*, 13–25.

Watanabe, N., Madaule, P., Reid, T., Ishizaki, T., Watanabe, G., Kakizuka, A., Saito, Y., Nakao, K., Jockusch, B.M., and Narumiya, S. (1997). p140mDia, a mammalian homolog of Drosophila diaphanous, is a target protein for Rho small GTPase and is a ligand for profilin. EMBO J. *16*, 3044–3056.

Wiesner, S., Helfer, E., Didry, D., Ducouret, G., Lafuma, F., Carlier, M.F., and Pantaloni, D. (2003). A biomimetic motility assay provides insight into the mechanism of actin-based motility. J. Cell Biol. *160*, 387–398.

Xu, Y., Moseley, J.B., Sagot, I., Poy, F., Pellman, D., Goode, B.L., and Eck, M.J. (2004). Crystal structures of a Formin Homology-2 domain reveal a tethered dimer architecture. Cell *116*, 711–733.

Yang, H.C., and Pon, L.A. (2002). Actin cable dynamics in budding yeast. Proc. Natl. Acad. Sci. USA *99*, 751–756.

Zigmond, SH. (2004). Formin-induced nucleation of actin filaments. Curr. Opin. Cell Biol. *16*, 99–105.

Zigmond, S.H., Evangelista, M., Boone, C., Yang, C., Dar, A.C., Sicheri, F., Forkey, J., and Pring, M. (2003). Formin leaky cap allows elongation in the presence of tight capping proteins. Curr. Biol. *13*, 1820–1823.